Appl. Phys. A 87, 599–605 (2007)
DOI: 10.1007/s00339-007-3879-y

Applied Physics A
Materials Science & Processing

Invited paper

T. WANG[1,2]
X. WANG[2,✉]
J. GUO[2]
Z. LUO[1]
K. CEN[1]

Characterization of thermal diffusivity of micro/nanoscale wires by transient photo-electro-thermal technique

[1] State Key Laboratory of Clean Energy Utilization, Zhejiang University Hangzhou, 310027, P.R. China
[2] Department of Mechanical Engineering, N104 Walter Scott Engineering Center, University of Nebraska-Lincoln, Lincoln, NE, 68588-0656, USA

Received: 26 October 2006/Accepted: 6 January 2007
Published online: 16 March 2007 •

ABSTRACT In this work, a transient photon-electro-thermal (TPET) technique based on step laser heating and electrical thermal sensing is developed to characterize the thermophysical properties of one-dimensional micro/nanoscale conductive and nonconductive wires. In this method, the to-be-measured thin wire/tube is suspended over two electrodes and is irradiated with a step cw laser beam. The laser beam induces a transient temperature rise in the wire/tube, which will lead to a transient change of its electrical resistance. A dc current is applied to the sample, and the resulting transient voltage variation over the wire is measured and used to extract the thermophysical properties of the sample. A 25.4-μm thick Pt wire is used as the reference sample to verify this technique. Sound agreement is obtained between the measured thermal diffusivity and the reference value. Applying the TPET technique, one can measure the thermal diffusivity of conductive single-wall carbon nanotube (SWCNT) bundles and nonconductive cloth fibers. For nonconductive wires, a thin ($\sim$ nm) metallic film is coated on the outside of the wire for electrical thermal sensing. The measured thermal diffusivity for the SWCNT bundle is 2.53×10^{-5} m^2/s, much less than the thermal diffusivity of graphite in the layer direction. For microscale cloth fibers, our experiment shows its thermal diffusivity is at the level of 10^{-7} m^2/s.

PACS 78.20.Nv; 42.62.-b; 65.80+n; 66.30.Xj

1 Introduction

In recent years, characterizing the thermophysical properties of materials at micro/nanoscales has received considerable attention due to the demand of developing reliable micro/nanoscale mechanical and electrical devices/systems. In the past, many methods have been well developed to measure the thermal properties of thin films. Limited experimental approaches have been developed for investigation of the thermophysical properties of one-dimensional micron/nanostructures [1]. As the main measurement techniques to obtain thermophysical properties of materials in such low dimensions and small scales, the 3ω method [2, 3] and microfabricated devices method [4, 5] have been widely used. The thermal conductivity of individual carbon nanotubes (CNTs) has been measured using the 3ω method [6, 7] and microfabricated devices method [8, 9].

For the techniques reviewed above, the 3ω method provides a compelling means to characterize the thermal conductivity of CNTs with sound accuracy. In this technique, the wire/tube itself serves as a heater and at the same time as a temperature sensor. Feeding an ac current at frequency ω through the sample will generate a temperature fluctuation at 2ω, and accordingly an electrical resistance variation at 2ω. Considering the ω frequency current through the sample, the 2ω resistance variation will give rise to a 3ω voltage fluctuation across the sample. This 3ω voltage fluctuation is tightly related to the heat transfer in the sample and can be used to extract its thermophysical properties. However, this technique requires the sample endowed with linear I–V behavior. Meanwhile, CNTs have both metallic and semiconductive properties, depending on their chirality indexes (n, m) [10]. The 3ω technique can only be applied to metallic CNTs. For many semiconductive one-dimensional micro/nanoscale structures, the 3ω technique cannot be applied. For the microfabricated devices method, suspended structures are fabricated, and micrometer-long samples are used to bridge the two suspended islands. Joule heat is created on the heater island to result in heat transfer to the other island through the wire/tube. The thermal conductivity of the sample can be calculated based on measured temperature difference between the two suspended islands and the heat transfer rate.

Motivated to develop a fast technique that can measure the thermophysical properties of a wide spectrum of micro/nanoscale wires, we have developed in this paper a transient photo-electro-thermal (TPET) technique based on step laser heating and electrical thermal sensing. In this technique, a step cw laser beam is employed to heat the wire/tube, and a very small dc current is used to detect the thermal response of the sample. The optical heating source easily ensures constant heating power in the wire and clean signal for sampling. This technique can be applied to both conductive and nonconductive materials and takes a very short time for measurement (less than 1 s). For nonconductive wires/tubes, a thin Au film is coated on the wire surface for electrical thermal sensing. In Sect. 2, the experimental principles and

✉ Fax: 402-472-1465, E-mail: xwang3@unl.edu

physical model development are presented. The experimental details and results are discussed in Sect. 3.

2 Experimental principles and physical model development

2.1 *Experimental principles*

In the TPET experiment, the to-be-measured wire is suspended between two copper electrodes. The wire is irradiated with a cw laser beam as shown in Fig. 1. The laser spot is large enough to cover the entire wire and portion of the bases. Upon the constant power laser heating, the wire will have a temperature rise and reach steady state in a short time. How fast/slow the temperature of the wire reaches steady state is directly related with its thermal diffusivity. For instance, wires with small thermal diffusivity will take a long time to reach the steady state. This temperature rise history can be detected and used to determine the thermal diffusivity of the wire. In the experiment, because of its temperature change, the resistance of the wire will change with time as well. The size of the electrodes is much larger than the diameter of the wire. This ensures that, due to the huge heat sink effect of the electrodes, the temperature change of the bases by laser heating is much smaller than that of the wire. As a result, the resistance variation of the bases due to laser irradiation will be negligible compared with that of the wire. In order to detect the resistance variation of the wire, a dc current is passed through it. Consequently, a small voltage change can be sensed across the wire. When the wire has a moderate temperature increase, it is physically reasonable to assume that the voltage change is proportional to the temperature rise. In the experiment, only the information about how fast the voltage increases to reach steady state is needed. No knowledge about the real temperature rise is required.

In the experiment, part of the laser pulse irradiates the electrodes, which could increase the temperature of the electrodes and change their electrical resistance. On the other hand, this effect is negligible compared to the resistance change of the one-dimensional nanostructure. This is because the dimensions of the bases are much larger (several orders of magnitude) than the diameter of the wire, ensuring that the temperature change of the bases by laser heating is much smaller than that of the wire. In addition, the electrical resistance of the electrode bases is much smaller than that of the wire. Consequently, the resistance variation of the bases due to laser irradiation will be negligible in the experiment.

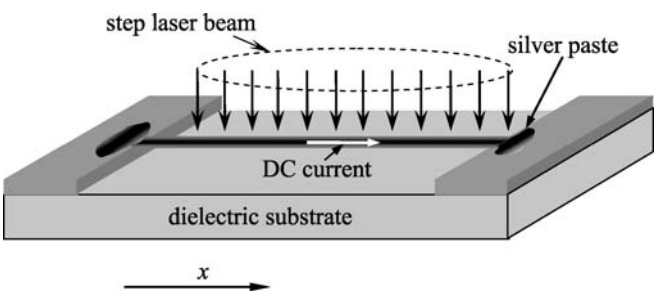

FIGURE 1 Schematic of the experimental principle for the TPET technique

2.2 *Physical model development*

In the experiment, the time taken for the wire to reach steady state is much longer than the characteristic thermal diffusion time ($\mu = r_0^2/(2\alpha)$, where r_0 and α are the radius and thermal diffusivity of the wire, respectively) across the wire cross-section. Therefore, it is physically reasonable to assume that the wire has a uniform temperature distribution in its cross-section during the experiment. Only the heat transfer along the axial direction of the wire needs to be considered. In the experiment, the output power of the laser is maintained constant. For the heat transfer in the wire along the axial direction, the governing equation is

$$\varrho c_\mathrm{p} \frac{\partial T}{\partial t} = k \frac{\partial^2 T}{\partial x^2} + (\dot{g} + g') \,, \tag{1}$$

where $\dot{g}$ and g', in the unit of $\mathrm{W\,m^{-3}}$, are the heating induced by the laser beam and the dc current passing through the wire. ϱ, c_p, k and T are the density, specific heat, thermal conductivity, and temperature of the wire, respectively.

The solution to (1) consists of two parts: the transient component θ that reflects the temperature rise due to laser heating, and the steady temperature T_t due to the very small electric heating (g'). This electrical current is always fed through the wire, even before the laser irradiates the wire.

Due to the linear feature of the equation, the temperature elevation by the laser heating can be described

$$\varrho c_\mathrm{p} \frac{\partial \theta}{\partial t} = k \frac{\partial^2 \theta}{\partial x^2} + \dot{g} \,, \tag{2}$$

where $\theta = T - T_\mathrm{t}$. At the beginning of laser heating, θ is zero along the wire. At both ends of the wire, its temperature takes a constant value of T_0 since the copper electrodes are an excellent conductor and can be treated as large heat sinks. Therefore, θ is zero at both ends of the wire. It needs to be pointed out that in (2) the laser beam is assumed uniform over the wire. In fact, there is a distribution of the laser beam along the wire. The effect of the nonuniformity of the laser beam is discussed in the next section.

Equation (2) can be solved using the Green function method [11]. The Green function of the partial differential is

$$G_{X11}\left(x, t \,|x', \tau\right) = \frac{2}{L} \sum_{m=1}^{\infty} \mathrm{e}^{-m^2\pi^2\alpha(t-\tau)/L^2} \times \sin\left(m\pi \frac{x}{L}\right) \sin\left(m\pi \frac{x'}{L}\right) \,, \tag{3}$$

where $\alpha = k/\varrho c_\mathrm{p}$ is the thermal diffusivity of the wire, and L is its length.

The solution to (3) is expressed as

$$\theta(x, t) = \frac{\alpha}{k} \int_{\tau=0}^{t} \int_{x'=0}^{L} G_{X11}(x, t|x',)\dot{g}\, \mathrm{d}x'\, \mathrm{d}\tau \,. \tag{4}$$

The resistance change of the wire due to temperature rise is what we intend to measure in the experiment. This resistance variation reflects the change of the average temperature of the

wire, which is expressed as

$$\bar{\theta}(t) = \frac{1}{L}\int_{x=0}^{L} \theta(x,t)\,\mathrm{d}x = \frac{8\dot{g}L^2}{k}\sum_{m=1}^{\infty}\frac{1}{(2m-1)^4\pi^4} \times \left(1-\mathrm{e}^{-(2m-1)^2\pi^2\alpha t/L^2}\right). \quad (5)$$

2.3 *Methods for data reduction*

From (5) – the solution to the thermal diffusion equation, it can be seen that in addition to the heating power and length of the sample, the temperature curve is only related with the Fourier number $F_0 = at/L^2$. At the steady state (when $t \to \infty$), the average temperature rise of the wire due to laser heating is $\bar{\theta}_s = \dot{g}L^2/12k$. Using this temperature rise as the reference, we can normalize the average temperature increase of the wire as

$$\theta_{\mathrm{norm}} = \frac{\bar{\theta}(t)}{\bar{\theta}_s} = \sum_{m=1}^{\infty}\frac{96}{(2m-1)^4}\left(1-\mathrm{e}^{-(2m-1)^2\pi^2\alpha t/L^2}\right). \quad (6)$$

Considering the linear relationship among the temperature rise, resistance change, and voltage variation over the wire, the voltage variation measured in the experiment can represent the evolution of the normalized temperature.

Based on the normalized temperature evolution, two methods are designed and employed in this work to determine the thermal diffusivity of the sample. One method uses the characteristic point of the temperature evolution curve. The characteristic point is a special point that has the highest sensitivity to the thermal diffusivity change. This feature can be described as that $\Delta\theta_{\mathrm{norm}}\Delta t$ has the maximum value when the thermal diffusivity changes by $\Delta\alpha$, where $\Delta\theta_{\mathrm{norm}} = \partial\theta_{\mathrm{norm}}/\partial\alpha\Delta\alpha$ and $\Delta t = \partial t/\partial\alpha\Delta\alpha$. This requires $\partial\theta_{\mathrm{norm}}/\partial\alpha\partial t/\partial\alpha$ has the maximum value at the characteristic point. Based on (6), it is not difficult to find this point has a value of 0.8665 for θ_{norm}, and the corresponding Fourier number is 0.2026, which is shown in Fig. 2 (point C is the characteristic point). In the characteristic point method, the characteristic time (Δt_c) is identified from the $T \sim t$ curve when the normalized temperature rise reaches 0.8665. The thermal diffusivity of the wire can be determined as $\alpha = 0.2026L^2/\Delta t_c$.

The other method for determining the thermal diffusivity of the material is global data curve fitting. In this fitting, using (6), different values of the thermal diffusivity of the sample are used to calculate the theoretical temperature evolution. The thermal diffusivity is determined from a least-square fit to the normalized temperature. This method is very useful in the experiment because it can substantially reduce the effect of noise in the experimental data.

2.4 *Effect of nonuniform distribution and finite rising time of the laser beam*

In (2) as discussed above, the laser beam is assumed uniform over the entire wire while in practice there is a nonuniform distribution. The intensity profile of the diode laser beam ($\lambda = 809$ nm) used in our experiment can be approximated as a Gaussian distribution [12]. In order to find out to what extent the curve fitting method is affected by the nonuniformity of the laser beam, the laser energy distribution along the wire is assumed linear from its middle point to its end. The laser energy at the middle of the wire is assumed two times the energy at the end of the wire. The linear assumption of energy distribution provides an extreme situation. In real experiments, the laser energy distribution over the wire will be much more uniform, especially for short wires irradiated with a large laser beam spot. Numerical simulations are conducted to study the temperature evolution with considering the nonuniform laser distribution.

Another issue comes from the rising time of the laser beam. In practice, there is a finite rising time from the startup to the steady laser energy output, which can be seen in Fig. 3. For the laser beam in our experiment, there is a sharp rise for the laser energy at the starting point, but it still takes about 10 μs to reach the steady state. In our numerical study, the energy level of the laser beam is assumed to have a linear increase from $t = 0$ to the rising time t_r of 10 μs

Considering the laser energy distribution and the rising time, the governing equation for the heat transfer along the

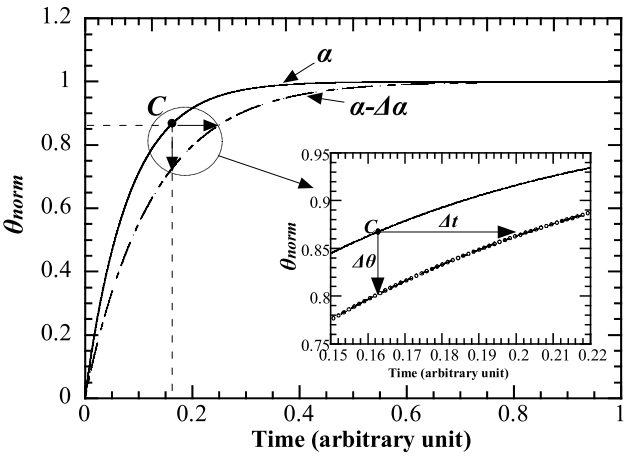

FIGURE 2 Schematic for characteristic point determination and physical explanation

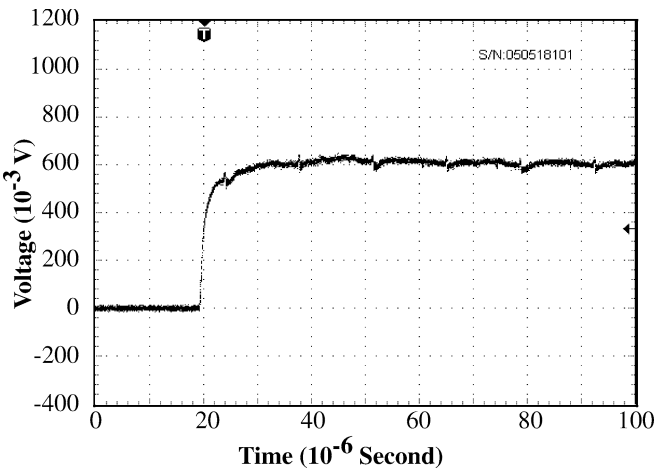

FIGURE 3 Measured rising time of the laser beam used in our experiment

	platinum wire	polyester
length (mm)	0.77	0.302
density (kg/m^3)	2.145×10^4	1.368×10^3
specific heat (J/kg K)	133	1.20×10^3
thermal conductivity (W/m K)	71.6	0.36
calculated thermal diffusivity (m^2/s)	2.51×10^{-5}	2.19×10^{-7}

TABLE 1 Properties of Pt and polyester wires used in the calculation

wire is expressed as

$$\frac{\partial(\varrho c_\mathrm{p} T)}{\partial t} = k\frac{\partial^2 T}{\partial x^2} + Q' \times \left(1 + \frac{2x}{L}\right), \quad (x < L/2), \qquad (7)$$

where Q' is the laser induced heating power at the end of the wire. This parameter is equal to a constant value Q_0 when $t > t_\mathrm{r}$ and is $Q_0 t/t_r$ when $t < t_\mathrm{r}$.

To explore how the nonuniform distribution of the laser and its rising time influence the temperature rise of the wire, calculations are conducted for a Pt wire that has high thermal diffusivity and one type of polyester with low thermal diffusivity. The properties of the polyester [13] and Pt wires [14] are summarized in Table 1. Their length takes the typical values used in our experiment. Our numerical calculation shows that the nonuniform distribution and the rising time of the laser beam in the TPET experiment can be neglected. Our experimental results using Pt wires also confirm this point, and will be discussed in Sect. 3. The radiation heat loss from the wire surface is negligible for microfibers. Detailed study about the radiation effect can be found in work by Wang's group [3, 12].

3 Experimental details and results

3.1 *Experimental set up*

The TPET experiment (shown in Fig. 4) uses an infrared diode laser (BWTEK BWF-2, 809 nm wavelength) for heating purpose. The laser beam passes through a collimator and is directed by a focal lens to the to-be-measured wire. A dc voltage is applied to the Wheatstone bridge circuit, where the wire (R_w) is used as one arm of the bridge circuit. R_1, R_2, R_3 are adjustable rheostats with very low resistance-temperature coefficient, ensuring the detected voltage variation is caused by the wire. A digital phosphor oscilloscope (Tektronix TDS7054, maximum sampling rate 5 GS/s) is connected to the bridge to detect the transient voltage change of the wire. In order to reduce the ac noise from the ambient, a series of batteries are connected to supply the dc voltage and shield cables are used to connect the circuit. To minimize the influence from air convection, the wire is housed in a vacuum chamber where the pressure is maintained at a level below 1×10^{-3} Torr. In the experiment, the laser heating time and digital phosphor oscilloscope's sampling time are chosen to ensure the rising curve of the voltage is fully developed and captured.

At the beginning of the experiment, a very small current is fed through the bridge to make it balanced by adjusting the resistors in the circuit. Then the wire is suddenly irradiated with a constant laser beam while the small electrical current is still going through the circuit. A temperature change will occur in the wire. This temperature change will induce some resistance change of the wire. Consequently, the balance of the Wheatstone bridge will be destroyed, and a voltage change will be detected. This unbalanced voltage change over time is recorded in the oscilloscope. The rising curve of the voltage can be used to determine the thermophysical properties of the sample.

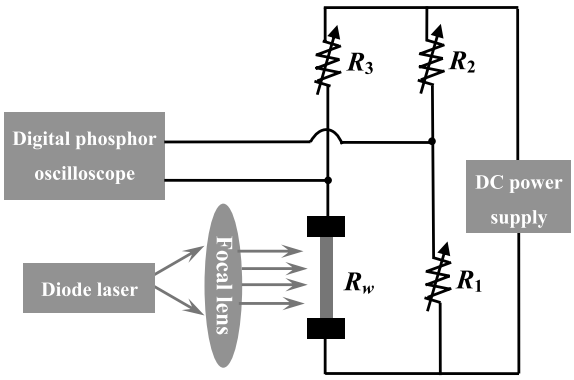

FIGURE 4 Schematic setup for the TPET experiment

3.2 *System calibration*

In order to verify the TPET technique and the theoretical model developed in Sect. 2, a 25.4 μm thick and 5.07 mm long platinum wire is characterized. The experimental conditions, such as the applied laser power, dc current through the wire, and the results of fitting are listed in Table 2. The visible size of the laser spot is around 10 mm. Figures 5 and 6 show the fitting result in comparison with the experimental data. In Fig. 5, considering the experimental uncertainty, the data points whose normalized temperature increase in the range of 3σ around 0.8665 are linearly fitted to find the characteristic point. σ is the normalized standard deviation when the rising curve reaches its steady state, and is 1.87×10^{-2} for this experiment. The oscillation in the data shown in Fig. 5 is attributed to the experimental noise, mainly introduced by the system when the oscilloscope picks up signals from the electrical circuit. When determining the critical point, linear fitting in the area around the critical point can significantly suppress the uncertainty induced by this data oscillation. The thermal diffusivity determined based on the characteristic point method is 2.45×10^{-5} m^2/s, and the characteristic time is 0.213 s. In Fig. 6 for global data curve fitting, the root mean square (RMS) between the experimental data and theoretical fitting is calculated as

	Pt wire	CNT bundle
length (mm)	5.074	0.771
resistance of sample (Ω)	1.3	208.9
dc current (mA)	14.7	0.68
laser power (W)	4.0	1.2
α by characteristic point method (m^2/s)	2.45×10^{-5}	2.52×10^{-5}
α by global data curve fitting (m^2/s)	2.45×10^{-5}	2.53×10^{-5}
RMS of global data curve fitting	2.30×10^{-2}	3.12×10^{-2}

TABLE 2 Details of experimental conditions for the Pt wire and SWCNT samples characterized in the experiment

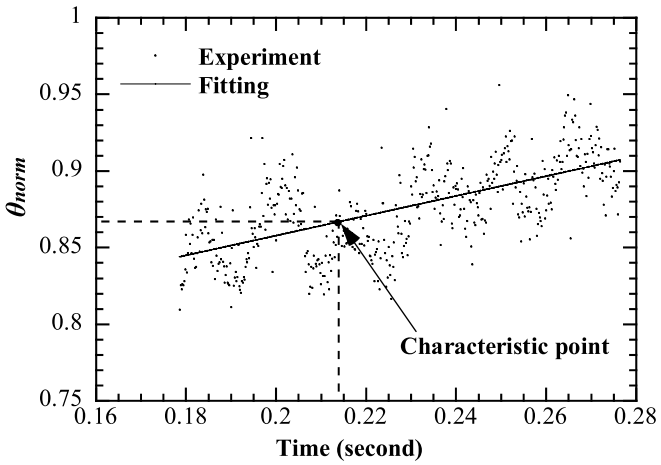

FIGURE 5 Characteristic point fitting for the Pt wire experiment

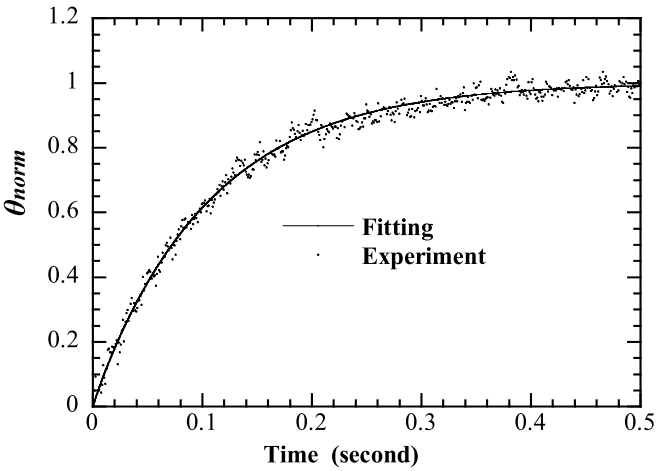

FIGURE 6 Global curve fitting of the experimental data for thermal diffusivity determination for the Pt wire

$\text{RMS} = \sqrt{\sum_{i}^{N} (V_i - V_{\text{theo},i})^2 / N}$, where N, V_i and $V_{\text{theo},i}$ denote the number of experimental data points, normalized voltage of experiment, and normalized value of fitting, respectively. The result by global data fitting is $2.45 \times 10^{-5}\,\text{m}^2/\text{s}$ with the RMS of 2.30×10^{-2}. It is quite consistent with the result of the characteristic point method and close to the literature value of $2.51 \times 10^{-5}\,\text{m}^2/\text{s}$ [14].

3.3 *Thermal characterization of* SWCNT *bundles*

In this section, bundles consisting of SWCNTs are measured using the established TPET technique and the developed solution. Ropes of well-aligned SWCNTs centimeters long were synthesized using an H_2/Ar arc discharge method. The synthesis process is described in detail in work by Liu et al. [15]. The structural quality and thickness of these SWCNT bundles were reported in our recent work using Raman scattering and SEM [16]. The typical thickness/diameter of the SWCNT bundle is measured to be around 60 μm and various-size pores exist in the bundle. The orientation of the SWCNTs does not follow the axial direction of the bundle. A Raman scattering study shows that the primary diameter of

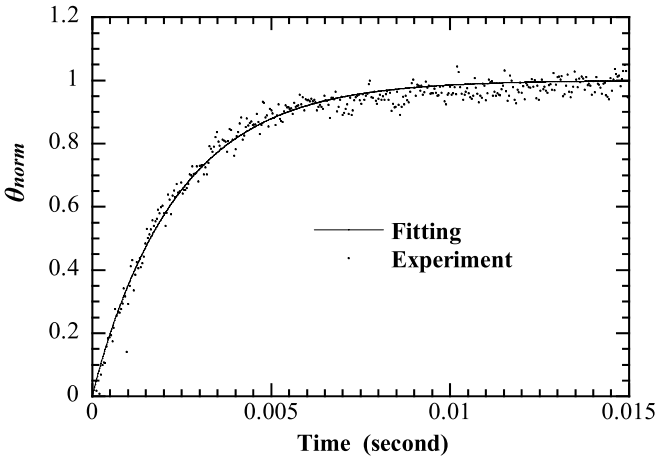

FIGURE 7 The global data fitting for the SWCNT bundle

SWCNTs in the bundle is 1.75 nm [16]. Therefore, the bundle is comprised of many SWCNTs.

In the experiment, the SWCNT bundle is connected between two copper electrodes using silver paste. Table 2 shows the length and resistance of the SWCNT bundle measured in the experiment. The laser power, dc current through the wire, and the results of fitting are also summarized in Table 2. Figure 7 shows the global data fitting against the normalized experimental result. Using the characteristic point method and global data fitting, one finds the thermal diffusivity of the SWCNT bundle to be $2.52 \times 10^{-5}\,\text{m}^2/\text{s}$ and $2.53 \times 10^{-5}\,\text{m}^2/\text{s}$, respectively. It is clear that the two methods give close results. Compared with the work by Hou et al. [12], our measurement result is close to that for CNT #1 sample ($2.98 \times 10^{-5}\,\text{m}^2/\text{s}$) in their work. The deviation in thermal diffusivity for different samples is probably attributed to different alignment of the tube bundles and tube–tube interaction, as discussed in the work of Hou et al. [12]. The SWCNT bundles measured in this work has much lower thermal diffusivity ($\sim 1.9\%$ of that for graphite in the layer direction). This significantly reduced heat transfer is probably due to the random orientation of SWCNTs in the bundle, the finite thermal contact resistance between SWCNT threads, and structural defects in the SWCNTs themselves.

3.4 *Thermal characterization of cloth fiber*

For nonconductive wires, the TPET technique cannot be directly applied since no electrical thermal sensing is feasible. To sense the temperature variation of the wire, the wire is coated with a very thin Au film. In the experiment, it is physically reasonable assuming that the wire has a uniform temperature distribution over its cross-section. Therefore, the temperature of the metallic coating represents that of the wire. The cloth fiber is carefully suspended on one Cu electrode, and silver paste is used to fix the wire on the electrode. After the silver paste dries, the wire is fixed on another electrode using silver paste and the mechanical contact is strengthened at the same time. The sample is placed in a sputter coating machine to coat a very thin Au film ($\sim$ nm) on the surface of the sample after the silver paste is dry. In order to improve the electrical contact between the coated fiber and the elec-

trodes, silver paste is carefully spread at the edges of the Cu electrodes near the connecting point after Au coating. After the Au film is coated, the sample is studied using an SEM. The cloth fiber we measured is a single wire, confirmed by our SEM study. The SEM observation shows the cloth fiber-poly (ethylene terephthalate) studied in this work has a diameter of 10.4 μm and length of 0.59 mm. The coated cloth fiber is measured to have a resistance of 319 kΩ. The Wheatstone bridge is balanced and a 3.0 V dc voltage is applied over the bridge. In this experiment, the output power of the diode laser is 1.20 W. The thermal diffusivity of the cloth fiber is determined as $5.00 \times 10^{-7}\,\mathrm{m^2/s}$ and $5.29 \times 10^{-7}\,\mathrm{m^2/s}$ using the characteristic point method and global data curve fitting. In order to estimate the uncertainty of the global data curve fitting, several measurements are conducted using the same sample, and the repeatability for global fitting is found to be $^{+0.13}_{-0.09} \times 10^{-8}\,\mathrm{m^2/s}$. Figure 8 shows the global data fitting result, which agrees well with the experimental data.

For thermal characterization of nonconductive wires, the measured α is an effective value that includes the effect of the thin metallic coating. The real thermal diffusivity of the wire could be extracted based on the measurement result and the concept of thermal conductance. The effect of the coated Au film can be ruled out using the concept of thermal conductance. The thermal conductance (G_f) of the thin film coating is defined as $G_\mathrm{f} = A_\mathrm{f} k_\mathrm{f}/L$, where k_f and A_f are the thermal conductivity of the film in the axial direction and cross-sectional area of the thin film, respectively. This equation cannot be directly used to evaluate the thermal conductance of the metallic thin film since its cross-sectional area A_f is difficult to measure. In addition, k_f is different from that of bulk metal, and is difficult to characterize. In our work, G_f is evaluated using the Wiedemann–Franz law, which relates the thermal conductivity of metal (k) to its electrical conductivity (σ) as $L_\mathrm{Lorenz} = k/(\sigma T)$. The Lorenz number L_Lorenz for Au has weak dependence on temperature ($2.35 \times 10^{-8}\,\mathrm{W\,\Omega/K^2}$ at 0 °C and $2.40 \times 10^{-8}\,\mathrm{W\,\Omega/K^2}$ at 100 °C [17]). Based on the Wiedemann–Franz law, the thermal conductance of the thin film coating can be readily calculated based on the measured electrical resistance of the wires as $G_\mathrm{f} = L_\mathrm{Lorenz} T/R$.

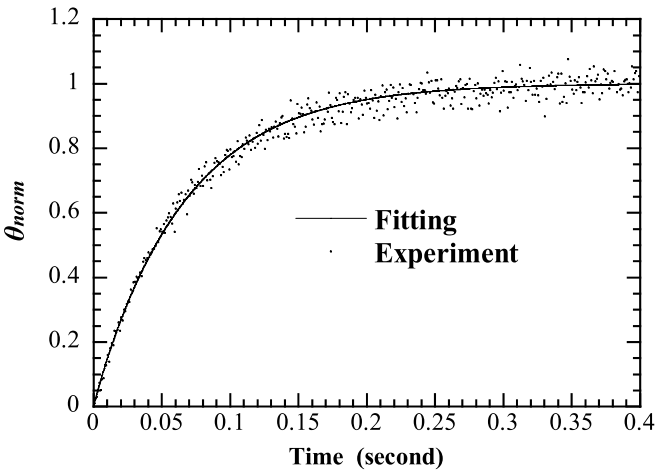

FIGURE 8 The global data fitting result for the cloth fiber versus the normalized experimental data

In our experiment, the measured data of effective thermal diffusivity of the cloth fiber has combined contribution from the wire and Au coating, which can be defined as

$$\alpha_\mathrm{eff} = \frac{k(1-\beta) + k_\mathrm{f}\beta}{\varrho c_\mathrm{p}(1-\beta) + \varrho_\mathrm{f} c_\mathrm{p,f}\beta}\,, \tag{8}$$

where ϱ_f and $c_\mathrm{p,f}$ are the density and specific heat of Au coating; $\beta = A_\mathrm{f}/A_e$ is the cross-area ratio of Au coating over coated wire, and A_e is the cross-sectional area of wire with Au coating. Since $\beta \ll 1$, $c_\mathrm{p,f}\beta \ll \varrho c_\mathrm{p}(1-\beta)$ and $1-\beta \cong 1$). The real thermal diffusivity of the wire is calculated as

$$\alpha = \alpha_\mathrm{eff} - \left(\frac{L_\mathrm{Lorenz} T}{R}\frac{L}{A_\mathrm{w}}\right) \Big/ (\varrho c_\mathrm{p})\,. \tag{9}$$

The amended term is calculated as

$$\Delta\alpha = \alpha_\mathrm{eff} - \alpha = \left(\frac{L_\mathrm{Lorenz} T}{R}\frac{L}{A_\mathrm{w}}\right) \Big/ (\varrho c_\mathrm{p})\,. \tag{10}$$

Following this amendment and using the density and specific heat of polyester ($\varrho = 1.368 \times 10^3\,\mathrm{kg\,m^{-3}}$, $c_\mathrm{p} = 1.20 \times 10^3\,\mathrm{J\,kg^{-1}K^{-1}}$) [13], the amended item is calculated as $\Delta\alpha = 9.39 \times 10^{-11}\,\mathrm{m^2/s}$, which is negligible compared with the thermal diffusivity of the wire. This is attributed to the very thin thickness of the Au coating. Another advantage of big resistance (or thin thickness) of coating is to reduce the effect of contact resistance. Although the real electrical resistance of the Au coating is less than the value measured in the experiment, the effect of electrical contact resistance will become small when the Au coating has a large electrical resistance.

During the measurement, the temperature of the sample will increase. To evaluate the exact temperature rise becomes difficult due to the small size of the sample and lack of knowledge about the thermal conductivity of the sample and laser beam absorption. On the other hand, some first order estimations can still be done to give a general idea about temperature increase. Our estimation suggests that for the Pt wire, the initial temperature before laser heating with the electrical current going through is about 3 °C higher than the ambient, and the temperature rise due to laser heating is not beyond 30 °C. As for the cloth fiber, the initial temperature before laser heating when the current is going through is about 10 °C higher than the ambient, and the temperature rise due to laser heating is not beyond 50 °C.

In this work, the TPET technique is applied to measure various one-dimensional μm-thick samples. For thermal characterization of wires with diameters in the nanometer range, several important issues deserve careful technical consideration. The first one is the radiation heat loss from the wire surface. For a wire, the ratio of radiation heat transfer from the wire surface to the heat conduction along the wire is approximately proportional to $\varepsilon(T^4 - T_0^4)L^2/[k_\mathrm{e}(T-T_0)D]$. It is evident that when the diameter (D) becomes smaller, the radiation heat transfer becomes more important. In order to reduce the radiation heat transfer effect on the final measurement result, short wires several micrometers in length are preferred. It is estimated that for the cloth fiber measured in our experiment, if its diameter is 50 nm, a 20–30 μm or

shorter sample is needed to reduce the radiation effect. The second issue for measuring nanometer-thick wires is the requirement for fast laser heating. Since short samples are required to measure nanometer-thick wires, the time taken for the sample to reach steady state will be very short, could be a few microseconds or shorter. To make the rising time of the laser beam have negligible effect on this fast temperature evolution, the laser beam should have a short rising time ($\sim$ ns). Such a short rising time can be achieved using fast optical switches to control the laser beam. The third issue is the electrical contact between the wire and electrode. In this work, the electrical contact between the wire and electrode is enhanced using silver paste. For nanometer wires, a much improved technique is needed. Focused ion beam deposition of Pt [7] provides a better way to enhance the electrical contact between the nanowire and electrode. The fourth issue is related to non-conductive nanowires. For single nonconductive nanowires, (9) cannot be used since the thickness of the metallic coating is comparable to the wire thickness. β in (8) is difficult to determine and can no longer be ignored. To solve this problem, noncontact thermal sensing technologies without using metallic coatings is preferred, such as measuring the change of the scattering light from the nanowire or observing the peak shift in its Raman spectrum.

4 Conclusion

In this work, a technique based on transient optical heating and electrical thermal sensing was developed to characterize the thermal transport in one-dimensional microstructures. Compared with the 3ω technique, the developed TPET technique features much stronger signal and substantially reduced experimental time. This technique has the capability of characterizing a wide variety of conductive and non-conductive micro/nanoscale wires/tubes. Applying this technique, we measured the thermal diffusivity of a platinum wire to be $2.45 \times 10^{-5}\,\mathrm{m}^2/\mathrm{s}$, agreeing well with the reference value. In addition, we measured the thermal diffusivity of a SWCNT bundle. The measurement result was $2.53 \times 10^{-5}\,\mathrm{m}^2/\mathrm{s}$, much smaller than that of graphite in the layer direction. Applying the TPET technique, we characterized the thermal diffusivity of microscale nonconductive wires successfully.

ACKNOWLEDGEMENTS This work was supported by National Science Foundation (CMS:0457471), Nebraska Research Initiative, Air Force Office for Scientific Research, and MURI from ONR. SWCNT bundles were provided by Chang Liu and Huiming Cheng from Shenyang National Laboratory for Materials Science, Chinese Academy of Sciences. The authors especially appreciate the strong support from the China Scholarship Council for the State Scholarship Fund to pursue the research.

REFERENCES

1 J. Hou, X. Wang, C. Liu, H. Cheng, Appl. Phys. Lett. **88**, 1910 (2006)
2 L. Lu, W. Yi, D.L. Zhang, Rev. Sci. Instrum. **72**, 2996 (2001)
3 P. Vellelacheruvu, Experimental research on thermal transportation in individual one-dimensional micro/nano structure, M.S. Thesis, University of Nebraska-Lincoln (2006)
4 P. Kim, L. Shi, A. Majumdar, P.L. McEuen, Phys. Rev. Lett. **87**, 215 502 (2001)
5 L. Shi, D. Li, C. Yu, W. Jang, D. Kim, Z. Yao, P. Kim, A. Majumdar, J. Heat Transf. **125**, 881 (2003)
6 T.Y. Choi, D. Poulikakos, J. Tharian, U. Sennhauser, Appl. Phys. Lett. **87**, 013 108 (2005)
7 T.Y. Choi, D. Poulikakos, J. Tharian, U. Sennhauser, Nano Lett. **6**, 1589 (2006)
8 C. Yu, L. Shi, Z. Yao, D. Li, A. Majumdar, Nano Lett. **5**, 1842 (2005)
9 M. Fujii, X. Zhang, H. Xie, H. Ago, K. Takahashi, T. Ikuta, H. Abe, T. Shimizu, Phys. Rev. Lett. **95**, 065 502 (2005)
10 M.S. Dresselhaus, G. Dresselhaus, P.C. Eklund, *Science of Fullerenes and Carbon Nanotubes* (Academic Press, San Diego, 1996)
11 J. Beck, K. Cole, A. Haji-Sheikh, B. Litkouhi, *Heat Conduction Using Green's Functions* (Hemisphere, New York, Appendix X, 1992), p. 482
12 J. Hou, X. Wang, J. Guo, J. Phys. D Appl. Phys. **39**, 3362 (2006)
13 L. Olenka, E.N. da Silva, W.L.F. Santos, E.C. Muniz, A.F. Rubira, L.P. Cardoso, A.N. Medina, L.C.M. Miranda, M.L. Baesso, A.C. Bento, J. Phys. D Appl. Phys. **34**, 2248 (2001)
14 F.P. Incropera, D.P. Dewitt, *Heat and Mass Transfer*, 5th edn. (Wiley, New York, 2002), p. 907
15 C. Liu, H.M. Cheng, H.T. Cong, F. Li, G. Su, B.L. Zhou, M.S. Dresselhaus, Adv. Mater. **12**, 1190 (2000)
16 J. Hou, X. Wang, J. Guo, P. Vellelacheruvu, J. Appl. Phys. **100**, 124 314 (2006)
17 C. Kittel, *Introduction to Solid State Physics*, 5th edn. (Wiley, New York, 1976), p. 178